Consequences of nonlinear heat transport laws on expected plasma profiles

K. Lackner

IPP 5/14 March 1987

MAX-PLANCK-INSTITUT FÜR PLASMAPHYSIK

8046 GARCHING BEI MÜNCHEN

MAX-PLANCK-INSTITUT FÜR PLASMAPHYSIK

GARCHING BEI MÜNCHEN

Consequences of nonlinear heat transport laws on expected plasma profiles

K. Lackner

IPP 5/14 March 1987

Die nachstehende Arbeit wurde im Rahmen des Vertrages zwischen dem Max-Planck-Institut für Plasmaphysik und der Europäischen Atomgemeinschaft über die Zusammenarbeit auf dem Gebiete der Plasmaphysik durchgeführt.

Abstract für IPP 5/14

Die zu erwartete Variation der Plasmadruckprofile bei Veränderung der Leistungsdeposition in Tokamaks wird für ein einfaches lineares und ein quadratisches Wärmeleitungsgesetz untersucht. Es wird gezeigt, daß die bei einem quadratischen Gesetz folgende Versteifung der resultierenden Profile ausreicht, um innerhalb der zu erwartenden Fehlerschranken das experimentell beobachtete Phänomen der "Profilkonsistenz" ohne weitere Annahme nichtlokaler Effekte zu erklären.

Consequences of nonlinear heat transport laws on expected plasma profiles.

K. Lackner
Max-Planck Institut für Plasmaphysik, Euratom Association
D-8046 Garching

1.Introduction:

Tokamak experiments with pure Ohmic heating and with additional heating in the L-regime have demonstrated a remarkable resilience of electron temperature profiles against changes in power deposition profiles and plasma density. This observation has been termed profile consistency, and was frequently interpreted as a proof of the nonlocal nature of plasma transport processes in tokamaks.

This interpretation has been challanged recently in workshops/1/, where it was in particular pointed out that local but nonlinear heat transport laws could also lead to a stiffening in the response of temperature profiles to power deposition changes. Obviously this possibility has so far not been explored in a sufficiently broad way and its ultimate verification should involve detailed statistical analysis of the experimental data. As most of the discussion surrounding profile consistency so far has been led however in an only partly quantitative way and mostly relied on visual comparison between properly normalized $T_e(r)$ profiles, we also restrict ourselves here to illustrate in a similar way the expected variations under the simplest heat transport law compatible with global L-mode scaling.

2. Transport models considered

For the stated purpose of a rather qualitative illustration we make a number of simplifying assumption which otherwise would have to be viewed critically. So we do not distinguish between electron and ion transport (assuming $T_e = T_i$). We use in the following calculations two heat transport models, a linear one

$$q_{heat} = - f_1(r) \cdot \nabla p \qquad ...(1)$$

the quadratic one

$$q_{heat} = f_2(r) \cdot (\nabla p)^2 \qquad ...(2)$$

with f_1 and f_2 chosen as $f_1(r) = f_2(r) = (1 + (r/a)^2)^3$. Only relative varitions will be considered, so that no absolute coefficient values need to be specified. (q_{heat} ..radial heat flux density).

Both transport laws satisfy automatically the observed independence of global confinement times from density, but the choice of pressure gradient rather than e.g. $n \cdot \nabla T$ to enforce this reflects at this instance only convenience (it avoids having to specify in each case separately the density profiles). A quadratic law like equ. (2) could also be considered as a local equivalent to Goldston's L-mode scaling. Choice of f_2 as

$$f_2(r) = c \cdot r^2 \frac{q^2}{B_t^2}$$

would in fact lead to

$$\tau_E \sim \frac{I_p}{\sqrt{P_{heat}}} R^{1.5} a^{-.5}$$

with close similarity to the confinement fit proposed in /2/. (q ..local safety factor, R ..plasma major radius, a ..plasma minor radius, B_t ..toroidal field, I_p ..toroidal plasma current). As this local heat transport would vanish at the axis, it would have to be supplemented by an additional, nonvanishing contribution.

3. Results for specific power deposition cases

To give first a general impression we have carried out a comparison using two idealized, rather extreme model cases: one with a peaked, triangular and one with a completely flat power deposition profile. The most pronounced differences between the predicted pressure profiles would arise for both transport models in the central region, which in the usual discussion about profile consistency would however be excluded as presumably dominated by sawtooth transport. The resilience of the outer zones is of course a simple consequence of the fact that q_{heat} and therefore the pressure gradients at any value of r are determined by the total power deposited (and not radiated away) within this radius, which, under the conditions used in this comparison (same total power) have to approach each other for the two cases near the boundary. In the usual way of assessing the resulting changes - profiles normalized to their values at half radius - visible changes in the outer regions would appear only in the linear (fig.1a) but hardly in the quadratic transport law case (fig.1b). Even more resilient to deposition profile changes are global confinement times, which are a third integral over the power deposition profile, and in addition weight the pressures with the volume element. For the cases shown, the difference in deposition would lead to a change of 50% in τ_E for the linear, and of 20% for the quadratic law assumed.

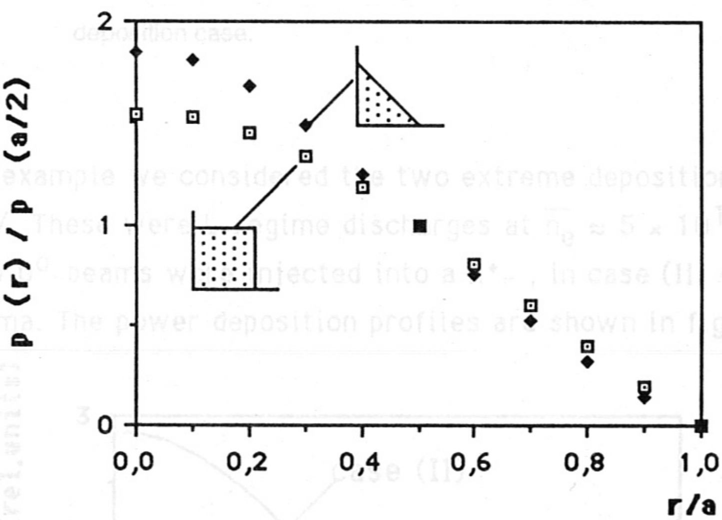

Fig. 1a: normalized pressure profiles as predicted by the linear law for a rectangular and a triangular deposition case.

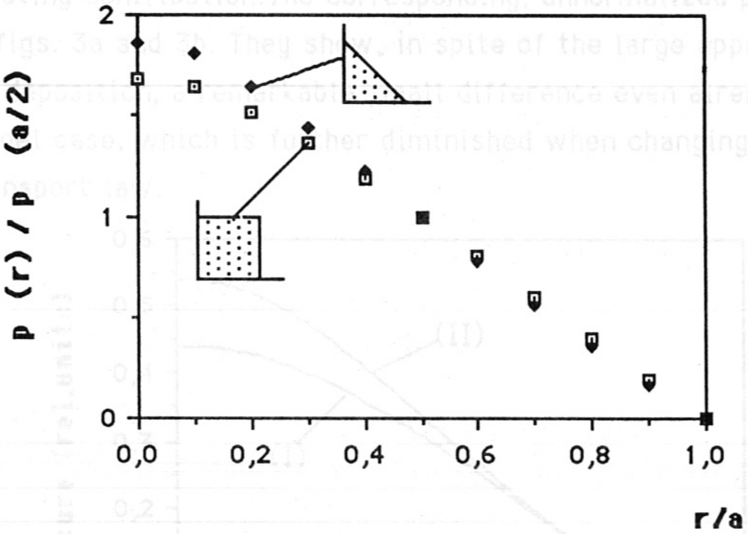

Fig. 1b: normalized pressure profiles as predicted by the quadratic law for a rectangular and a triangular deposition case.

As a realistic example we considered the two extreme deposition profile cases reported in /3/. These were L-regime discharges at $\overline{n_e} \approx 5 \times 10^{19} m^{-3}$, where in case (I) 29 kev D^0-beams were injected into a H^+- , in case (II) 42 kev H^0-beams into a D^+-plasma. The power deposition profiles are shown in fig. 2, and include

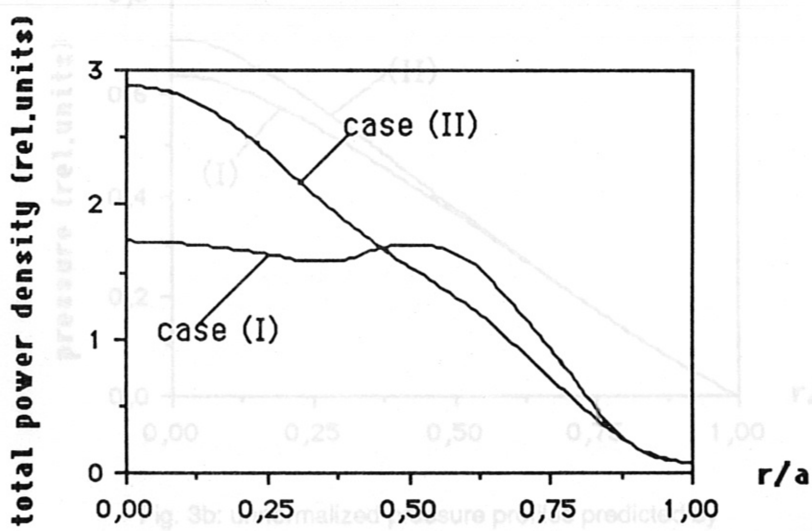

Fig.2: total power deposition profile for the two extreme cases reported in /5/.

the Ohmic heating contribution.The corresponding, unnormalized pressure profiles are given in figs. 3a and 3b. They show, in spite of the large apparent difference in the power deposition, a remarkable small difference even already for the linear transport model case, which is further diminished when changing over to the quadratic transport law.

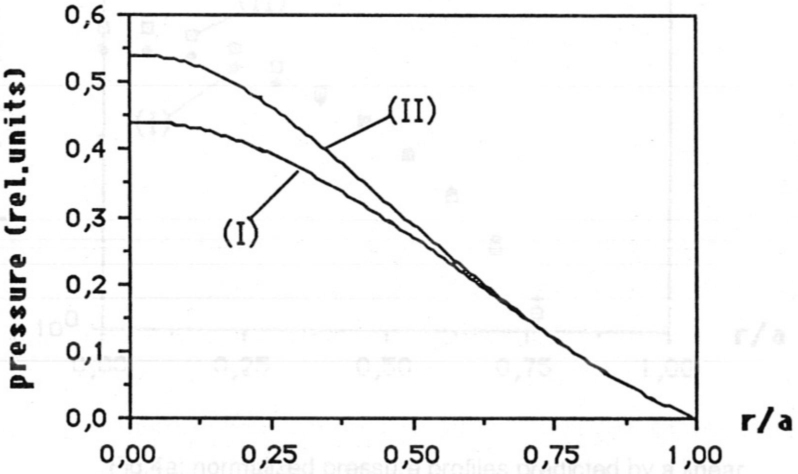

Fig. 3a: unnormalized pressure profiles predicted by the linear transport law for the power deposition cases of fig.2.

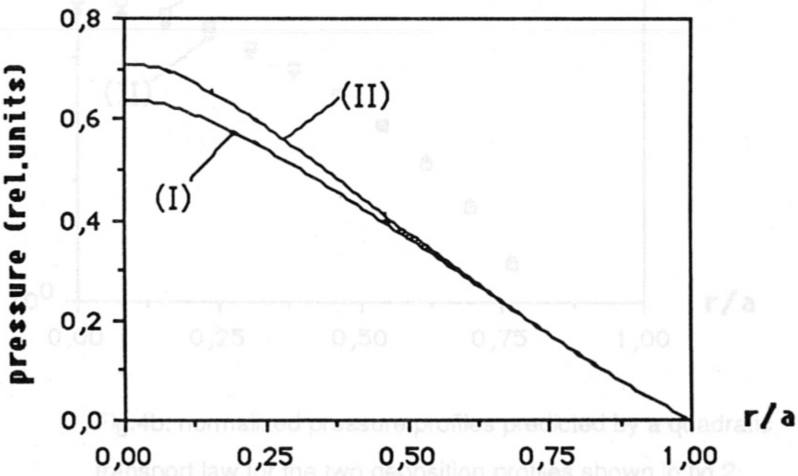

Fig. 3b: unnormalized pressure profiles predicted by the quadratic transport law for the power deposition cases of fig.2.

For this case we have plotted results also in the logarithmic fashion used in /4/ (figs.4a and 4b).

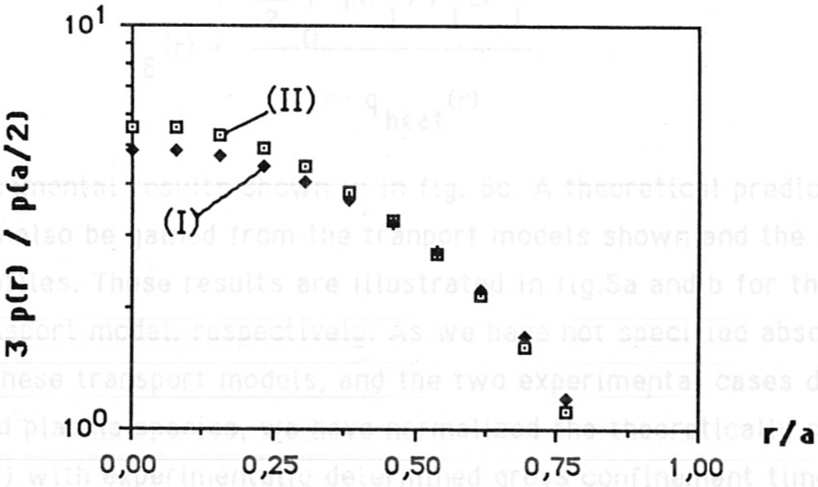

Fig.4a: normalized pressure profiles predicted by a linear transport law for the two deposition profiles shown in fig.2.

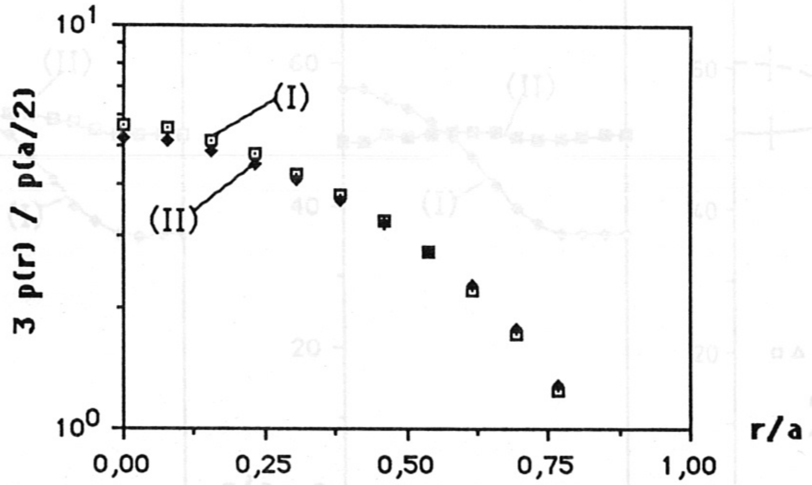

Fig.4b: normalized pressure profiles predicted by a quadratic transport law for the two deposition profiles shown in fig.2.

Again it becomes clear that outside the central regions, variations expected in the case of the quadratic transport law would be hidden by the error bars.

The experimental results of ref./3/ were discussed in terms of a so-called local energy confinement time, defined as

$$\tau_E(r) = \frac{\frac{3}{2}\int_0^r p(r_1)\, r_1\, dr_1}{r \cdot q_{heat}(r)}$$

with the experimental results shown in in fig. 5c. A theoretical prediction for this parameter can also be gained from the tranport models shown and the given deposition profiles. These results are illustrated in fig.5a and b for the linear and quadratic transport model, respectively. As we have not specified absolute constants in these transport models, and the two experimental cases differ also in the background plasma species, we have normalized the theoretically computed values of $\tau_E(r)$ with experimentally determined gross confinement times $\tau_E(a)$. (The latter values are determined primarily by the known isotope effect on confinement, which swamps such small differences arising from deposition.)

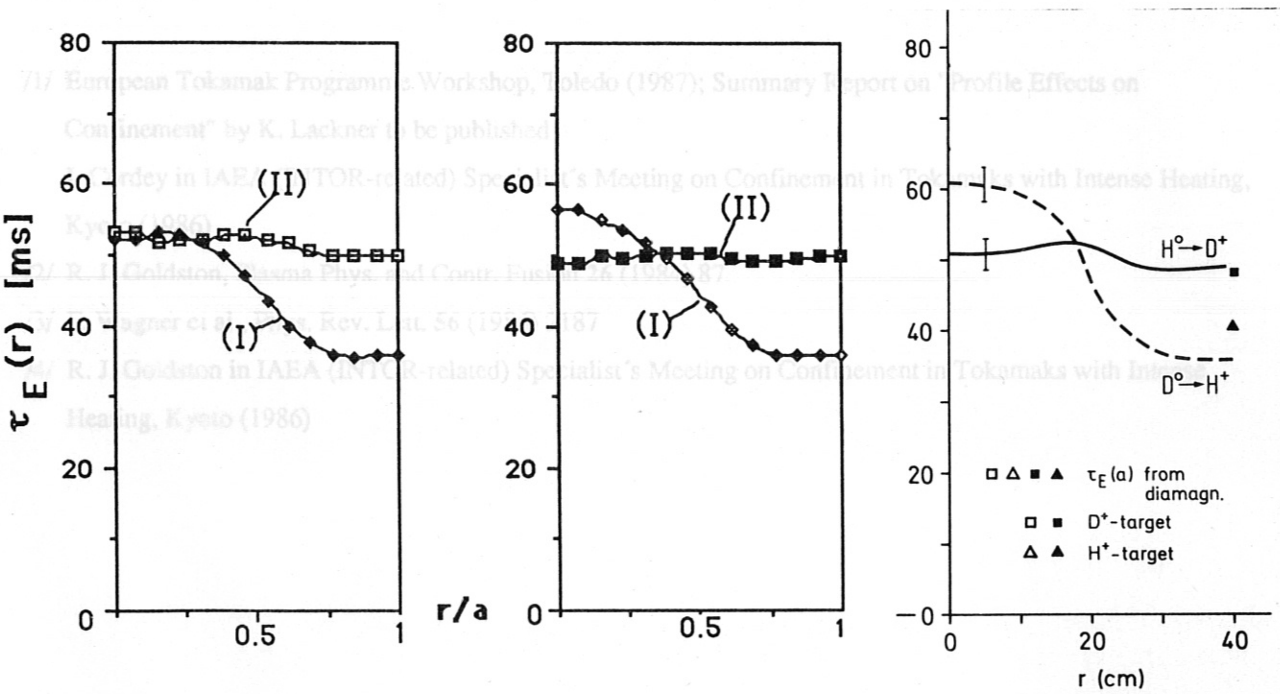

5a 5b 5c

Fig. 5: local energy confinement times as function of radius for the two power deposition cases of fig. 2, as measured experimentally (5c), and as predicted by the linear (5a) and quadratic (5b) transport laws,

4. Conclusions:

The above examples show that on the basis of presently available data it seems difficult to rule out a local, nonlinear transport law as an explanation of the observed profile resilience in tokamaks. A local transport law of the above form in fact automatically links profile resilience to confinement degradation with power. The considerations can of course not rigorously disprove the explanation of plasma profiles by some non-local principle. One so far unanswered argument in favour of such a more global explanation is the sharp transition between L and H-mode behaviour, and the non-existence of mixed situations with part of the plasma volume in one and part in the other regime.

References:

/1/ European Tokamak Programme Workshop, Toledo (1987); Summary Report on "Profile Effects on Confinement" by K. Lackner to be published
J. Cordey in IAEA (INTOR-related) Specialist´s Meeting on Confinement in Tokamaks with Intense Heating, Kyoto (1986)

/2/ R. J. Goldston, Plasma Phys. and Contr. Fusion **26** (1984) 87

/3/ F. Wagner et al., Phys. Rev. Lett. **56** (1986) 2187

/4/ R. J. Goldston in IAEA (INTOR-related) Specialist´s Meeting on Confinement in Tokamaks with Intense Heating, Kyoto (1986)